

Elimination of temperature cross-sensitivity for polymer FBG-based humidity sensor by gamma radiation treatment

Ivan Chapalo^{*a}, Andrei Gusarov^b, Karima Chah^a, Andreas Ioannou^c, Andreas Pospori^c, Ying-Gang Nan^a, Kyriacos Kalli^c, Patrice Mégret^a

^aElectromagnetism and Telecom Department, University of Mons, 31 Boulevard Dolez, Mons, Belgium 7000; ^bSCK-CEN, 200 Boeretang, Mol, Belgium 2400; ^cPhotonics and Optical Sensor Research Laboratory, Cyprus University of Technology, 33 Saripolou Street, Limassol, Cyprus 3036

ABSTRACT

In this work, we investigate the influence of gamma radiation treatment on sensing properties of fiber Bragg gratings (FBGs) inscribed in polymer CYTOP fiber with line-by-line method and femtosecond laser pulses. Polymer FBGs are known to have a wider strain range and a stronger temperature sensitivity compared to silica FBGs. Also, they exhibit sensitivity to the relative humidity (RH) that is therefore an additional physical quantity possible to measure. However, in practical applications of RH sensing, temperature cross-sensitivity must be compensated. Irradiating CYTOP FBG samples with various doses (80, 160, 200, 280, and 520 kGy), we found that the gamma radiation treatment changes their climatic properties. Initially positive value of the temperature sensitivity (19.6 pm/°C) decreases with the received dose with subsequent change of the sign from positive to negative. This opens a possibility of making FBGs insensitive to temperature. Among the irradiated samples, the one received the dose of 200 kGy demonstrated the lowest temperature sensitivity (1.77 pm/°C). For higher dose (520-kGy), the sensitivity was found to be -38.9 pm/°C. Along with a decrease of temperature sensitivity, we observed an increase of RH sensitivity with the received dose from 13.3 pm/%RH for pristine FBG up to 56.8 pm/%RH for the case of 520 kGy dose. Thus, by correct selection of the irradiation dose, gamma irradiation of CYTOP FBGs is a promising pre-treatment technique to improve the RH sensitivity of CYTOP FBGs with eliminating the temperature effect.

Keywords: Polymer optical fiber, fiber Bragg gratings, CYTOP, perfluorinated polymer, fiber optic sensors

1. INTRODUCTION

In recent years, perfluorinated polymer optical fibers (POFs) have been attracting significant attention from researchers due to their low attenuation in telecom transparency windows comparing to other POFs [1]. Besides telecom applications, various sensing principles which were well developed for silica fibers (for example, Brillouin and Rayleigh distributed sensing [2-3], intermodal interference sensing [4-5], and fiber Bragg gratings (FBGs) [6-7]), have been investigated for perfluorinated POFs as well [8-15]. Perfluorinated POFs are known to have a low photosensitivity, however the development of the direct FBG inscription method using a femtosecond laser pulses have been serving as an additional driver for the interest to this type of fiber [16]. Various applications of perfluorinated FBGs such as strain, RH and acoustic sensing have been investigated recently [14].

One research topic applied to perfluorinated POFs is the influence of ionizing radiation on their properties. The radiation induced attenuation (RIA) spectra during and after gamma irradiation of the POF samples were investigated to evaluate the ability of data transmission under gamma radiation conditions [17,18]. Also, the method of gamma radiation dosimetry based on the measurement of the RIA during (or after) irradiation was investigated [19]. Finally, the response of FBGs inscribed in perfluorinated POF was examined during and after irradiation [20,21]. Recently, we tested irradiated FBGs in the environmental chamber and we found that gamma radiation increases the sensitivity of perfluorinated FBGs to relative humidity (RH) and decreases their temperature sensitivity. In particular, among the applied dosed of 80, 120, 160 and 520 kGy, the FBG irradiated up to 160 kGy demonstrated the closest to zero temperature sensitivity [22]. This case is attractive for RH sensing since the temperature cross-sensitivity is minimized.

*ivan.chapalo@umons.ac.be

In this work, we apply additional doses of 200 and 280 kGy to previously investigated set of doses (80, 160 and 520 kGy) and we refine the dependences of temperature sensitivity on the irradiation dose. We also demonstrate that the dose of 200 kGy shows the closest to zero temperature sensitivity of $1.77 \text{ pm}/^\circ\text{C}$ among other doses. It also shows the RH sensitivity of $41.3 \text{ pm}/\% \text{RH}$ that is more than three times stronger than in the case pristine FBG.

2. EXPERIMENTAL SETUP

In experiments, we used a perfluorinated POF produced by Chromis Technologies. It had a custom design: a few-mode 20- μm CYTOP core and a 250- μm protective overclad were significantly less than the standard dimensions of CYTOP fiber (50, 62, 120- μm core and a 490- μm protective overclad). The reduced transversal size was aimed to increase the stability of the reflection spectrum (by reducing the number of reflected Bragg peaks). The fiber core had a gradient refractive index profile with effective refractive index of 1.34. A protective overclad was made of XYLEX material, which is a blend of polycarbonate and an amorphous polyester. FBGs were inscribed using a plane-by-plane direct inscription method by femtosecond laser [10, 11]. We used HighQ laser femtoREGEN source at $\lambda=517 \text{ nm}$ with 220 femtoseconds pulse duration and 1 kHz repetition rate. The fiber samples with FBGs were aligned and connected with standard silica SMF pigtailed using a UV-curing glue. Typical microscope image of the FBG (Zeiss Axio Imager.M2 microscope) and the reflection spectrum are presented in Figure. 1.

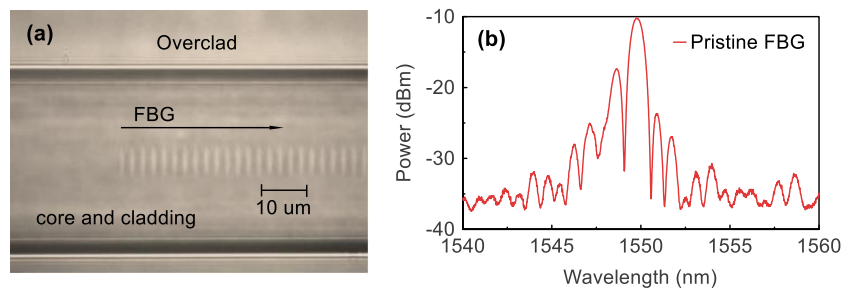


Figure 1. A transmission microscope image of the inscribed FBG (a) and a typical reflection spectrum of a pristine FBG (b).

Irradiation was conducted using a calibrated γ -radiation setup based on ^{60}Co irradiation sources located at a depth of seven meters in a water pool and provided a dose-rate of 5.3 kGy/h (Brigitte facility, SCK-CEN, Belgium, Figure 2 (b, c)). The irradiation sources formed a cylindrical volume where the stainless steel hermetic container with the fiber sample was placed for a specified time according to the required dose. Irradiation was conducted at a temperature of $41\text{-}44 \text{ }^\circ\text{C}$. Temperature was stabilized by an oven located at the hermetic container and controlled by the Eurotherm 2408 temperature controller.

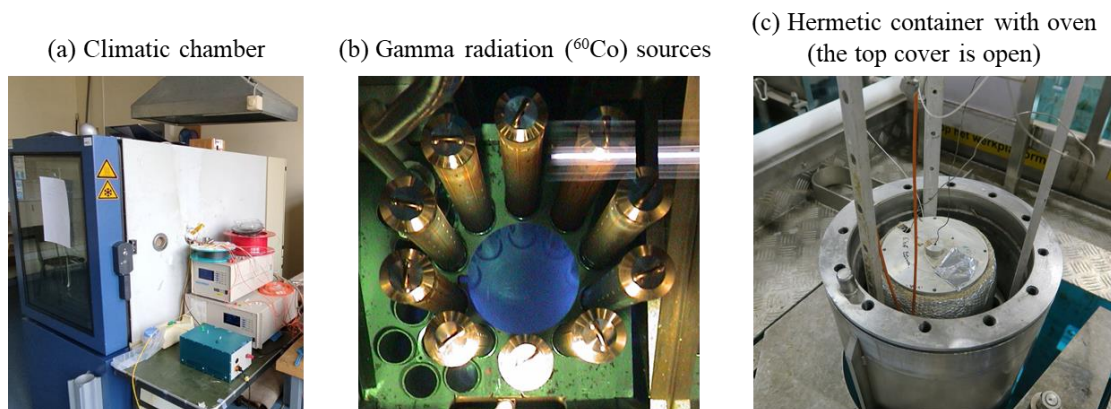


Figure 2. Photographs of the experimental facilities: the environmental chamber for climatic experiments (a) the irradiation sources (b), and the hermetic container for irradiation of the FBG samples (c).

Climatic experiments were conducted using an environment chamber Weiss SB22/300 (Figure 2 (a)). Temperature and RH were measured by the internal sensors of the chamber and by the Thorlabs TSP01 sensor for additional control.

Temperature annealing was performed for three hours (65°C, 40 %RH) prior to experiments to enhance the stability of the results and reduce possible hysteresis. We used a standard commercial interrogator (FiberSensing FS2200) operating in the 1500-1600 nm wavelength range for the monitoring of FBGs reflection spectra.

3. EXPERIMENTAL RESULTS

To investigate a temperature response of the pristine and irradiated FBG samples, we performed a temperature cycle at a humidity level of 40 % (Figure 3, lower part of the graph, right scale). The temperature was programmed to increase and then decrease stepwise with the values of 25, 35, 45, and 50 °C. The stabilization time at each temperature was 4 hours and the duration of temperature changes between adjacent stable values was 30 minutes. We measured the evolution of the Bragg wavelength (BW) of the pristine FBG and irradiated FBGs received gamma radiation doses of 80, 160, 200, 280, and 520 kGy. The evolution of the corresponding BW shift during the temperature cycle is presented in Figure 3 (upper part of the graph, left scale).

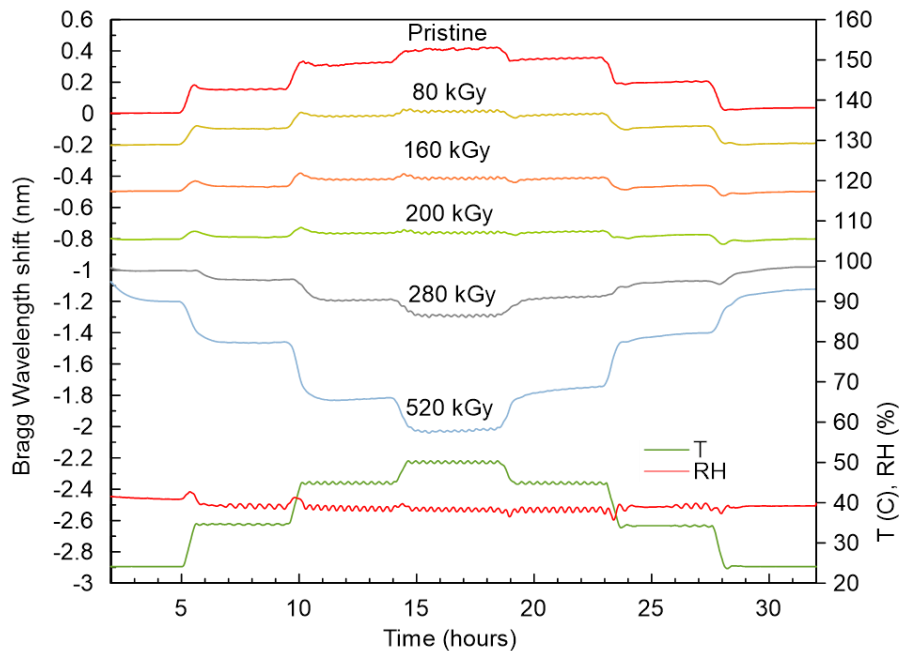


Figure 3. Temperature cycle for the pristine and irradiated FBGs: the temperature and RH graphs (bottom part of the graph, right scale) and the Bragg wavelength shift evolution (upper part of the graph, left scale. Offsets in the Bragg wavelength shift were introduced for better visibility).

The measured temperature sensitivities versus the irradiation dose are grouped in Table 1 and plotted in Figure 4. The pristine sample demonstrates the positive temperature sensitivity of 19.6 pm/°C. It is seen that the temperature sensitivity decreases with the irradiation dose with subsequent change of the sign. The FBGs that received the doses of 160 and 200 kGy demonstrate the closest to zero values (3.7 pm/°C and 1.77 pm/°C). These are the most interesting for practical applications cases since the temperature sensitivity is almost eliminated for the RH sensing. The last doses of 280 kGy and 520 kGy demonstrate negative sensitivities of -11.4 pm/°C and -38.9 pm/°C correspondingly. Figure 4 shows that the measured dependency can be well approximated by the linear law (with the slope of -0.1 (pm/°C)/kGy) if the last value of 520 kGy is not considered. It should be mentioned that we observed some instabilities in the Bragg wavelength evolution during the temperature and especially the RH experiments with the 520-kGy FBG: in some cases, the BW quickly changed (jumped) by several hundreds of picometers when the climatic parameters were stable. We assumed that such a behavior can be caused by very strong irradiation dose, which could provoke some physical damages in the material. These damages can be a reason of the instabilities in the FBG response. Also, a strong RH sensitivity of the 520-kGy FBG, providing a total BW change of more than three nanometers during RH cycles, could cause a sliding of the core/cladding structure inside the overclad. This could be another possible reason of the BW jumps in the case of 520 kGy. Taking the above into account, we excluded the sensitivity of the FBG with a 520 kGy received dose from a linear approximation.

Table 1. Temperature sensitivity versus received gamma radiation dose.

Irradiation dose (kGy)	Temperature sensitivity (pm/°C)
Pristine	19.6
80	8.3
160	3.7
200	1.77
280	-8
520	-38.9

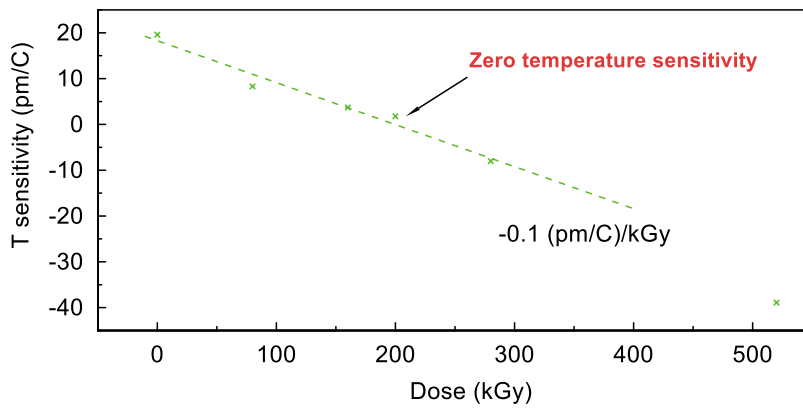


Figure 4. Dependency of FBG temperature sensitivity on the received gamma radiation dose.

Irradiated FBGs demonstrate not only a decrease of temperature sensitivity, but also a rise of RH sensitivity [22]. It rises from 13.3 pm/%RH for pristine FBG up to 56.8 pm/%RH for the case of 520 kGy dose. The 200-kGy dose, which provided the closest to zero temperature sensitivity, demonstrated the RH sensitivity of 41.3 pm/%RH. This is more than three times stronger comparing to the pristine FBG.

4. CONCLUSION

In this work, we investigated the dependency of temperature response on the irradiation dose for polymer FBGs inscribed in perfluorinated (CYTOP) fiber with XYLEX overclad. We added two new samples with 200 and 280 kGy received doses to refine the value of the irradiation dose necessary to eliminate the temperature sensitivity of the optical fiber. We showed a decrease of temperature sensitivity with irradiation dose. Moreover, the FBG received the 200-kGy dose showed minimum temperature sensitivity among other doses (1.77 pm/°C). It also demonstrated the RH sensitivity of 41.3 pm/%RH that is more than three times stronger comparing to the pristine FBG. Thus, irradiation of CYTOP FBGs by the optimal dose is prospective for RH sensing due to the increased RH sensitivity and the absence of temperature cross-sensitivity.

ACKNOWLEDGEMENTS

Fonds De La Recherche Scientifique – FNRS (T.0163.19 “RADPOF”). The research leading to these results has also received funding from the Horizon 2020 programme of the European Union (Marie Skłodowska-Curie Actions - Individual Fellowships) under REA grant agreement No. 844618 (project POSPORI). This work is also funded by the research project INTEGRATED/0918/0031 (LightSense Project) by the Republic of Cyprus through the Research and Innovation Foundation and European Development Fund and the Cyprus University of Technology.

REFERENCES

- [1] Koike, Y. and Asai, M. "The future of plastic optical fiber," *NPG Asia Materials* 1(1), 22-28 (2009).
- [2] Bai, Q *et al.* "Recent advances in Brillouin optical time domain reflectometry," *Sensors*, 19(8), 1862 (2019).
- [3] Liokumovich, L., Ushakov, N., Kotov, O., Bisyarin, M., Hartog, A. "Fundamentals of Optical Fiber Sensing Schemes Based on Coherent Optical Time Domain Reflectometry: Signal Model Under Static Fiber Conditions," *Journal of Lightwave Technology*, 33(17), 3660 – 3671 (2015).
- [4] Chapalo, I., Petrov, A., Bozhko, D., Bisyarin, M., Kotov, O. "Methods of signal averaging for a multimode fiber interferometer: An experimental study," *Proceedings of SPIE*, vol. 11028, 110282Q (2019).
- [5] Kotov, O., Chapalo, I. "Signal-to-noise ratio for mode-mode fiber interferometer," *Proceedings of SPIE*, vol. 10329, 1032945 (2017).
- [6] Safari Yazd, N, Chah, K., Caucheteur, C., Megret, P. "Comparison of regenerated fiber Bragg gratings properties in standard and B/Ge co-doped single-mode silica fibers," *Proceedings of IEEE Sensors*, 9278880 (2020).
- [7] Campanella, C.E., Cuccovillo, A., Campanella, C., Yurt, A., Passaro, V.M.N. "Fibre Bragg Grating Based Strain Sensors: Review of Technology and Applications," *Sensors*, 18(9), 3115 (2018).
- [8] Mizuno, Y., and Nakamura, K. "Potential of Brillouin scattering in polymer optical fiber for strain-insensitive high-accuracy temperature sensing," *Opt. Lett.*, 35(23), 3985–3987 (2010).
- [9] Mizuno, Y., Lee, H., Hayashi, N., Nakamura, K. "Noise suppression technique for distributed Brillouin sensing with polymer optical fibers," *Optics Letters*, 44(8), 2097-2100 (2019).
- [10] Liehr, S., Wendt, M., and Krebber, K. "Distributed strain measurement in perfluorinated polymer optical fibres using optical frequency domain reflectometry," *Measurement Science and Technology*, 21(9), 094023 (2010).
- [11] Mizuno, Y., Theodosiou, A., Kalli, K., Liehr, S., Lee, H., Nakamura, K. "Distributed polymer optical fiber sensors: a review and outlook," *Photonics Research*, 9(9), 1719-1733 (2021).
- [12] Chapalo, I., Theodosiou, A., Kalli, K., Kotov, O. "Multimode CYTOP fiber interferometer: an experimental study," *Proceedings of SPIE*, vol. 11199, 111990P (2019).
- [13] Chapalo, I., Theodosiou, A., Kalli, K., Kotov, O. "Multimode Fiber Interferometer Based on Graded-Index Polymer CYTOP Fiber," *Journal of Lightwave Technology*, 38(6), 1439-1445 (2020).
- [14] Theodosiou, A., and Kalli, K. "Recent trends and advances of fibre Bragg grating sensors in CYTOP polymer optical fibres," *Optical Fiber Technology*, 54, 102079 (2020).
- [15] Chah, K., Chapalo, I., Nan, Y.-G., Kinet, D., Megret, P., and Caucheteur, C. "800 nm femtosecond pulses for direct inscription of FBGs in CYTOP polymer optical fiber," *Optics Letters*, 46(17), 4272–4275 (2021).
- [16] Lacraz, A., Polis, M., Theodosiou, A., Koutsides C., and Kalli, K. "Femtosecond Laser Inscribed Bragg Gratings in Low Loss CYTOP Polymer Optical Fiber", *IEEE Photonics Technology Letters*, 27(7), 693-696 (2015).
- [17] Stajanca P. *et al.* "Effects of gamma radiation on perfluorinated polymer optical fibers," *Optical Materials*, 58, 226–233 (2016).
- [18] Chapalo, I., Gusarov, A., Kinet, D., Chah, K., Nan, Y.-G., Megret, P. "Postirradiation transmission characteristics of CYTOP fiber exposed by gamma radiation," *IEEE Transactions on Nuclear Science*, 69(4), 656-662 (2022).
- [19] Olusoji, O. J., Kam, W., and O’Keeffe, S. "Radiotherapy dosimetry based on perfluorinated polymer optical fibres," *Proceedings of SPIE*, 11354, 113541W (2020).
- [20] Broadway C. *et al.*, "CYTOP fibre Bragg grating sensors for harsh radiation environments," *Sensors*, 19(13), 2853 (2019).
- [21] Chapalo, I. *et.al.* "Online Gamma Radiation Monitoring Using Few-Mode Polymer CYTOP Fiber Bragg Gratings," *Sensors*, 23(1), 39 (2023).
- [22] Chapalo, I. *et.al.* "Gamma-radiation enhancement of sensing properties of FBGs in a few-mode polymer CYTOP fiber," *Optics Letters*, 48(5), 1248-1251 (2023).